Inorganic Chemistry

Article

pubs.acs.org/IC

Synthesis, Spectroscopic Properties, and Photoinduced CO-Release Studies of Functionalized Ruthenium(II) Polypyridyl Complexes: Versatile Building Blocks for Development of CORM–Peptide Nucleic Acid Bioconjugates

Caroline Bischof,[†] Tanmaya Joshi,[‡] Aakanksha Dimri,[§] Leone Spiccia,[‡] and Ulrich Schatzschneider*[,†,§]

[†]Lehrstuhl für Anorganische Chemie I, Ruhr-Universität Bochum, NC 3/74, Universitätsstrasse 150, D-44801 Bochum, Germany

[‡]ARC Centre of Excellence for Electromaterials Science and School of Chemistry, Monash University, Clayton, Victoria 3800, Australia

Supporting Information

ABSTRACT: A series of ruthenium(II) dicarbonyl complexes of formula $[RuCl_2(L)(CO)_2]$ (L = $bpy^{CH3,CH3}$ = 4,4′-dimethyl-2,2′-bipyridine, $bpy^{CH3,CHO}$ = 4′-methyl-2,2′-bipyridine-4-carboxyaldehyde, $bpy^{CH3,COOH}$ = 4′-methyl-2,2′-bipyridine-4-carboxylic acid, CppH = 2-(pyridin-2-yl)pyrimidine-4-carboxylic acid, dppzcH = dipyrido[3,2-a:2′,3′-c]phenazine-11-carboxylic acid), and $[RuCl(L)(CO)_2]^+$ (L = tpy^{COOH} = 6-(2,2′:6′,2″-terpyridine-4′-yloxy)hexanoic acid) has been synthesized. In addition, a high-yield synthesis of a peptide nucleic acid (PNA) monomer containing the 2-(pyridin-2-yl)pyrimidine ligand was also developed, and this compound was used to prepare the first Ru(II) dicarbonyl complex, $[RuCl_2(Cpp\text{-}L\text{-}PNA)(CO)_2]$,(Cpp-L-PNA = *tert*-butyl-*N*-[2-(*N*-9-fluorenylmethoxycarbonyl)aminoethyl]-*N*-[6-(2-(pyridin-2-yl)pyrimidine-4-carboxamido)hexanoyl]glycinate) attached to a PNA monomer backbone. Such metal-complex PNA–bioconjugates are attracting profound interest for biosensing and biomedical applications. Characterization of all complexes has been undertaken by IR and NMR spectroscopy, mass spectrometry, elemental analysis, and UV–vis spectroscopy. Investigation of the CO-release properties of the Ru(II) complexes in water/dimethyl sulfoxide (49:1) using the myoglobin assay showed that they are stable under physiological conditions in the dark for at least 60 min and most of them even for up to 15 h. In contrast, photoinduced CO release was observed upon illumination at 365 nm, the low-energy shoulder of the main absorption maximum centered around 300 nm, establishing these compounds as a new class of PhotoCORMs. While the two 2,2′-bipyridine complexes release 1 equiv of CO per mole of complex, the terpyridine, 2-(2′-pyridyl)pyrimidine, and dipyrido[3,2-a:2′,3′-c]phenazine complexes are less effective CO releasers. Attachment of the 2-(2′-pyridyl)pyrimidine complex to a PNA backbone as in $[RuCl_2(Cpp\text{-}L\text{-}PNA)CO_2]$ did not significantly change the spectroscopic or CO-release properties compared to the parent complex. Thus, a novel class of Ru(II)-based PhotoCORMs has been established which can be coupled to carrier delivery vectors such as PNA to facilitate cellular uptake without loss of the inherent CORM properties of the parent compound.

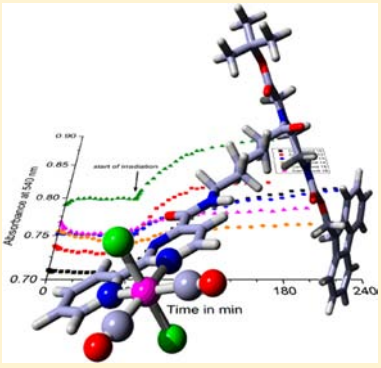

INTRODUCTION

In addition to nitric oxide (NO) and hydrogen sulfide (H_2S), carbon monoxide is now well established as the third gasotransmitter in higher organisms. Its biological activity shows a strong dose dependence. At high systemic concentrations, the typical signs of carbon monoxide poisoning which are also well known to the general public are due to its interference with oxygen transport and storage in the body as well as mitochondrial electron transfer which are affected by binding to heme proteins.[1] On the other hand, there is also a regular endogenous basal production of CO in healthy humans in the low micromolar concentration range, which serves an important function in cellular signaling and tissue protection.[2] This is mostly due to the activity of heme oxygenase-2 (HO-2), which is constitutively expressed in the liver, spleen, brain, and testes, among others.[3] In addition, there is also an inducible isoform of this enzyme (HO-1), which is upregulated in particular in response to oxidative stress.[4,5] A small amount of carbon monoxide is also generated by other processes.[6] Although it is generally assumed that, as in the case of nitric oxide, soluble guanylate cyclase (sGC) is the primary target of the signaling activity of carbon monoxide,[7−9] other systems have been recently identified which are significantly influenced by CO. In particular, modulation of ion channel gating by CO has received significant attention, although the mechanism is yet to be elucidated at a molecular level.[10] In order to utilize the important physiological function of carbon monoxide in human medicine,[11,12] the inherent difficulties in the application and dosage of this highly toxic gas have to be overcome. The strategy most commonly applied nowadays is the use of

Received: March 26, 2013
Published: August 6, 2013

   dx.doi.org/10.1021/ic400746n | *Inorg. Chem.* 2013, 52, 9297−9308

transition metal or main group carbonyl complexes as a solid storage form for carbon monoxide.

These CO-releasing molecules (CORMs) can easily be stored and handled and will only liberate the carbon monoxide in response to an external stimulus. This is usually achieved by a ligand exchange reaction with a solvent molecule upon dissolution in aqueous buffer,[13−24] but photoinduced CO release from a dark-stable prodrug is also possible in the so-called PhotoCORMs.[25−27] In addition to ruthenium(II) complexes, such as CORM-3 ([RuCl(glycinate)$(CO)_3$]) most commonly used in biological studies,[28] a number of other transition metal carbonyl complexes, mostly of iron,[29−33] manganese,[34−40] molybdenum,[22,23,41] cobalt,[21] rhenium,[42,43] and iridium,[44] have been introduced, but there is also a growing family of main group compounds now derived from sodium boranocarbonate $Na_2[H_3BCOO]$ CORM-A1.[45−48] An important parameter for potential therapeutic applications is the half-life for CO release, since ligand substitution reactions with water start immediately after dissolution in buffer and half-lives that are too short could well prevent CORMs from reaching their intended target sites in the body. In addition to activation of such CO-releasing molecules through ligand exchange, usually with water serving as the solvent, other processes to stimulate carbon monoxide release from metal carbonyl complexes have also been explored recently. For example, Schmalz et al. reported acyloxybutadiene iron tricarbonyl complexes which are stable in buffer under normal conditions, but enzymatic cleavage of the ester bond in these enzyme-triggered CO-releasing molecules (ET-CORMs) leads to a keto−enol tautomeric rearrangement which weakens the Fe−CO binding in $Fe(CO)_3$ leading to liberation of carbon monoxide.[31−33] In addition, light-induced CO release from metal−carbonyl complexes has been explored to achieve precise spatial and temporal control of carbon monoxide liberation. A number of such PhotoCORMs have been studied in the last couple of years which show promising biological activity.[26,27,30,34,35,37,49−56] However, an important issue in the development of novel PhotoCORMs is the choice of the metal−coligand combinations that allow photoexcitation at a wavelength where tissue penetration depth for the incident light is high.[57,58]

Thus, due to their similarity to hydrolytically activatable CORM-2 and -3 ($[RuCl(\mu\text{-}Cl)(CO)_3]_2$ and [RuCl(glycinato)$(CO)_3$], respectively), well-established synthetic chemistry, and tunable photophysical and photochemical properties, ruthenium(II) dicarbonyl complexes appeared to us as promising targets for development of novel PhotoCORMs.[59−61] Moreover, previous studies have already shown that such compounds can undergo photochemical decarbonylation.[62−66] Thus, in the present work, we report on the preparation, characterization, and CO-release studies of a series of ruthenium(II) dicarbonyl complexes of functionalized bi- or tridentate polypyridyl ligands. In addition, the carboxyl groups introduced will allow facile conjugation to delivery vectors for their targeted cellular uptake and controlled CO delivery.

As a proof-of-principle study, 2-(2′-pyridyl)pyrimidine-4-carboxylic acid (CppH) was therefore attached to a monomeric PNA backbone and used in the synthesis of the corresponding ruthenium(II) dicarbonyl complex followed by evaluation of the ruthenium(II) dicarbonyl dichloride-based PNA-like monomer for its CO-release activity.

EXPERIMENTAL SECTION

Chemicals. Ruthenium trichloride hydrate (Strem, Pressure Chemicals) and formic acid (Aldrich) were used without further purification. Other chemicals were either of reagent or analytical grade and used as purchased from commercial sources. Ligands and complexes, 6-(2,2′:6′,2″-terpyridine-4′-yloxy)hexanoic acid (**6**),[67] 4,4′-dimethyl-2,2′-bipyridine (**1**),[68] 4′-methyl-2,2′-bipyridine-4-carboxyaldehyde (**2**),[69] 4′-methyl-2,2′-bipyridine-4-carboxylic acid (**3**),[69] 2-(pyridin-2-yl)pyrimidine-4-carboxylic acid·HNO_3 (**4**),[70] dipyrido-[3,2-a:2′,3′-c]phenazine-11-carboxylic acid (dppzcH) (**5**),[71] *tert*-butyl *N*-[2-(*N*-9-fluorenylmethoxycarbonyl)aminoethyl] glycinate hydrochloride,[72] ethyl 6-aminohexanoate hydrochloride,[73] $[RuCl_2(CO)_2]_n$,[74] and $[RuCl_2(bpy^{CH3,COOH})(CO)_2]$ (**12**),[75] were synthesized according to literature procedures. All characterization data was in agreement with literature reports. Analytical-grade solvents were degassed by purging with dry, oxygen-free nitrogen for at least 30 min before use if necessary. Acetonitrile was dried by standing over calcium hydride overnight and *N*,*N*-dimethylformamide (DMF) by standing over activated 4 Å molecular sieves overnight. Deionized water was used for all reactions in aqueous solution. HPLC-grade solvents were used for all spectral studies.

Instrumentation and Methods. A vacuum line and Schlenk glassware were employed when reactions had to be carried out under an atmosphere of dry, oxygen-free dinitrogen, and assemblies were protected from light if necessary by wrapping them with aluminum foil. ^1H and ^1H broad-band decoupled ^{13}C NMR spectra were measured on Bruker DPX 200, AC 200, DPX 250, AM 300, and DRX 400 spectrometers using the signal of the deuterated solvent as the internal standard.[76,77] Chemical shifts δ are reported in parts per million (ppm) relative to tetramethylsilane ($Si(CH_3)_4$). Coupling constants *J* are given in Hertz. Abbreviations for the peak multiplicities are as follows: s (singlet), d (doublet), dd (doublet of doublets), ddd (doublet of doublet of doublets), t (triplet), and m (multiplet). EI and FAB mass spectra were measured on a VG Autospec instrument using 3-nitrobenzyl alcohol (3-NBA) as the matrix for the FAB measurements. ESI mass spectrometry was performed using either a Micromass Platform *II* with an ESI source (capillary voltage was 3.5 eV and cone voltage 35 V) or a Bruker Esquire 6000 spectrometer (solvent flow rate was 4 $\mu L \cdot min^{-1}$, nebulizer pressure of 10 psi, dry gas flow rate of 5 $L \cdot min^{-1}$, and dry gas temperature of 300 °C). Compounds were dissolved in an organic solvent and ionized using an electrospray ionization source (ESI). Ion peaks were compared with expected monoisotopic masses. In the assignment of the mass spectra, the most intense peak is listed. Infrared spectra were recorded on a Perkin-Elmer 1600 Series FTIR spectrometer or on a Bruker Tensor 27 IR spectrometer equipped with a Pike MIRacle Micro ATR accessory in the range of 500−4000 cm^{-1} with a resolution of ±4.0 cm^{-1}. Samples were measured as KBr disks or pure solids as indicated. Elemental analysis for organic compounds was performed with a VarioEL analyzer from Elementar Analysensysteme GmbH at the Ruhr-University Bochum, Germany. Elemental analyses of inorganic complexes were carried out at the Laboratory for Microanalytical and Thermal Analysis at the University Duisburg-Essen, Essen, Germany on a EA 1110 CE instrument or at the Campbell Microanalytical Laboratory, University of Otago, New Zealand. UV−vis absorption spectra were recorded on an Agilent 8453 diode array spectrophotometer in dimethyl sulfoxide or phosphate buffer solution (PBS). Thin layer chromatography (TLC) was performed using silica gel 60 F-254 (Merck) plates with detection of spots being achieved by exposure to iodine or UV light or using ninhydrin stain. Column chromatography was carried out using Silica gel 60 (0.040−0.063 mm mesh, Merck). Eluent mixtures are expressed as volume to volume (v/v) ratios.

Ligand Synthesis. Synthesis of ligands **7**, **8**, and **9** is described in the Supporting Information.

Complex Synthesis. *$[RuCl_2(bpy^{CH3,CH3})(CO)_2]$ (**10**).* This compound was synthesized by a slight modification to the procedure reported by Strouse and co-workers.[78] Under exclusion of dioxygen and light, $[RuCl_2(CO)_2]_n$ (0.115 g, 0.50 mmol) and 4,4′-dimethyl-

dx.doi.org/10.1021/ic400746n | Inorg. Chem. 2013, 52, 9297−9308

2,2′-bipyridine (**1**) (0.103 g, 0.56 mmol) were added to degassed methanol (5 mL). The reddish suspension obtained was heated in a CEM Discover microwave reactor to 100 °C for 2 min to yield yellow needles in a clear red solution. After storing the reaction vessel at 4 °C overnight, yellow needles of **10** were collected on a Buchner funnel, washed with a small amount of cold methanol, and dried in vacuo. Yield: 0.104 g (0.25 mmol, 50%). Anal. Calcd for $C_{14}H_{12}Cl_2N_2O_2Ru$ (M_r = 412.23): C, 40.79; H, 2.93; N, 6.80. Found: C, 41.37; H, 2.99; N, 6.81. IR (FT-ATR): ν 3065 (C−H_{arom}), 2958 (C−H_{aliph}), 2923 (C−H_{aliph}), 2058 (C≡O), 1986 (C≡O), 1651, 1484, 1445, 1403, 1381, 1302, 1245, 1139, 1038, 852, 836, 743, 634 cm^{-1}. ^1H NMR (400 MHz, $CDCl_3$): δ 9.00 (d, 2H, ^3J = 5.7 Hz), 8.00 (s, 2H), 7.44 (dd, 2H, ^3J = 5.6 Hz, ^4J = 0.9 Hz), 2.60 (s, 6H) ppm. ^{13}C NMR (101 MHz, $CDCl_3$): δ 196.05, 154.83, 152.55, 151.84, 128.21, 123.92, 21.74 ppm. MS (FAB$^+$, 3-NBA): m/z 412 $[M]^{\bullet+}$.

*[RuCl$_2$(bpy^{CH3,CHO})(CO)$_2$] (**11**).* Under exclusion of dioxygen and light, $[RuCl_2(CO)_2]_n$ (116 mg, 0.51 mmol) and 4′-methyl-2,2′-bipyridine-4-carboxyaldehyde (**2**) (110 mg, 0.55 mmol) were added to degassed tetrahydrofuran (5 mL). The bright yellow suspension obtained was heated in a CEM Discover microwave reactor to 80 °C for 30 min. After cooling the yellow suspension to 4 °C overnight, the yellow crude product was collected on a Büchner funnel and dried in vacuo for 1 h. The compound was purified by column chromatography on silica using ethyl acetate as the eluent under strict exclusion of light to prevent decomposition. Evaporation of the solvent afforded **11** as a yellow powder, which was dried in vacuo. Yield: 54 mg (0.13 mmol, 25%) (R_f = 0.39 in ethylacetate). Anal. Calcd for $C_{14}H_{10}Cl_2N_2O_3Ru{\cdot}2H_2O$ (M_r = 462.25): C, 36.38; H, 3.05; N, 6.06. Found: C, 37.03; H, 3.34; N, 5.04. IR (FT-ATR): ν 3070 (C−H_{arom}), 2962 (C−H_{aliph}), 2058 (C≡O), 1991 (C≡O), 1704 (C═O), 1620, 1562, 1476, 1447, 1379, 1260, 1236, 1178, 1091, 1017, 944, 849, 798, 743, 660, 631 cm^{-1}. ^1H NMR (400 MHz, $CDCl_3$) δ 10.23 (s, 1H), 9.44 (d, 1H, ^3J = 5.5 Hz), 9.03 (d, 1H, ^3J = 5.6 Hz), 8.59 (s, 1H), 8.16 (s, 1H), 8.02 (dd, 1H, ^3J = 5.5 Hz, ^4J = 1.2 Hz), 7.52 (d, 1H, ^3J = 4.8 Hz), 2.65 (s, 3H) ppm. As complex **11** is prone to (hemi)acetal formation and therefore only accessible in very low absolute yield, full characterization was not made.

*[RuCl$_2$(CppH)(CO)$_2$] (**13**).* CppH (**4**) (0.238 g, 0.90 mmol) was suspended in deoxygenated methanol (10 mL) and heated to 60 °C for 15 min to ensure complete dissolution. To the resulting clear solution, $[RuCl_2(CO)_2]_n$ (0.170 g, 0.746 mmol) was added, and the reaction mixture was heated to reflux under nitrogen for 2 h. During this time, dissolution of the ruthenium polymer was observed followed by precipitation of the product. The reaction mixture was cooled to 2 °C, and the precipitate was collected by filtration to yield **13** as a yellow solid. Yield: 0.200 g (0.466 mmol, 63%). Anal. Calcd for $C_{12}H_7Cl_2N_3O_4Ru{\cdot}H_2O$ (M_r = 447.19): C, 32.23; H, 2.03; N, 9.40. Found: C, 32.51; H, 2.11; N, 9.48. IR (KBr): ν 3096 (C−H_{arom}), 2757 (C−H_{aliph}), 2068 (C≡O), 2006 (C≡O), 1744 (C═O), 1618, 1578, 1554, 1426, 1251, 1208, 1026, 820, 766 cm^{-1}. ^1H NMR (200 MHz, DMSO-d_6): δ 9.81 (d, ^3J = 5.8 Hz, 1H), 9.31−9.28 (m, 1H), 8.88−8.83 (m, 1H), 8.51−8.43 (m, 1H), 8.31−8.28 (m, 1H), 8.06−7.99 (m, 1H) ppm. ^{13}C NMR (100 MHz, DMSO-d_6): δ 195.6, 195.4, 163.4, 162.9, 162.5, 156.6, 153.8, 151.6, 141.4, 130.3, 126.6, 122.8 ppm. MS (ESI$^-$): m/z 429.8 $[M - H]^-$.

*[RuCl$_2$(dppzcH)(CO)$_2$] (**14**).* $[RuCl_2(CO)_2]_n$ (0.170 g, 0.750 mmol) was suspended in deoxygenated methanol (15 mL) and heated to 60 °C for 15 min to complete dissolution. Dipyrido[3,2-a:2′,3′-c]phenazine-11-carboxylic acid (**5**) (0.293 g, 0.900 mmol) was added, and the reaction mixture was heated to reflux under nitrogen for 2 h. After cooling to 2 °C overnight, the precipitated product was collected by filtration, washed with cold methanol, and dried in vacuo to obtain **14** as a light brown solid. Yield: 0.360 g (0.649 mmol, 85%). Anal. Calcd for $C_{21}H_{10}Cl_2N_4O_4Ru{\cdot}MeOH$ (M_r = 586.35): C, 45.06; H, 2.41; N, 9.56. Found: C, 45.28; H, 2.25; N, 9.75. IR (KBr): 3064 (C−H_{arom}), 2946 (C−H_{aliph}), 2068 (C≡O), 2007 (C≡O), 1718 (C═O), 1633, 1418, 1359, 1235, 1177, 1051, 836, 762, 733 cm^{-1}. ^1H NMR (400 MHz, DMSO-d_6): δ 9.80−9.75 (m, 4H), 8.89−8.83 (m, 1H), 8.53−8.50 (m, 1H), 8.46−8.40 (m, 1H), 8.36−8.32 (m, 2H) ppm. ^{13}C NMR (100 MHz, DMSO-d_6): δ 196.6, 166.8, 156.0, 155.9, 148.5, 148.3, 143.8, 141.7, 141.1, 140.6, 136.9, 136.7, 131.8, 131.6, 130.4, 130.0, 128.6, 126.8 ppm. MS (ESI$^-$): m/z 554.8 $[M - H]^-$.

*[RuCl(CO)$_2$(tpy^{COOH})]PF$_6$ (**15**).* The compound was synthesized by a modified procedure of Gibson and co-workers.[79] $[RuCl_2(CO)_2]_n$ (0.286 g, 1.25 mmol) and 6-(2,2′:6′,2″-terpyridine-4′-yloxy)hexanoic acid (**6**) (0.499 g, 1.37 mmol) were suspended in ethanol/water (1:1 v/v) and heated to reflux for 3 h. Within the first 5 min, the color of the suspension changed from yellow to violet and then to black. Finally, a clear red solution was obtained, which was cooled to room temperature. Ammonium hexafluorophosphate (0.287 g, 1.76 mmol) dissolved in water (14 mL) was added dropwise to precipitate a beige solid from the red solution. After standing overnight, the solid had turned red and was collected by filtration and dried in vacuo. The crude product was dissolved in acetonitrile, layered with diethyl ether, and stored at 4 °C. Red crystals of **15** were precipitated over a period of 4 days, filtered off, and dried in vacuo. Yield: 0.409 g (0.58 mmol, 47%). Anal. Calcd for $C_{23}H_{21}ClF_6N_3O_5PRu{\cdot}EtOH$ (M_r = 746.99): C, 40.20; H, 3.64; N, 5.63. Found: C, 40.45; H, 3.24; N, 6.31. IR (KBr): ν 3084 (C−H_{arom}), 2943 (C−H_{aliph}), 2868 (C≡O), 2076 (C≡O), 2013 (C≡O), 1704 (C═O), 1607, 1562, 1478, 1429, 1364, 1219, 1165, 1095, 1064, 830, 787, 754 cm^{-1}. ^1H NMR (400 MHz, DMSO-d_6): δ 8.90 (d, 2H, ^3J = 5.3 Hz), 8.87−8.83 (m, 2H, ^3J = 8.3 Hz), 8.46 (s, 2H), 8.41−8.36 (m, 2H), 7.82−7.75 (m, 2H), 4.46 (t, 2H, ^3J = 6.4 Hz), 2.29 (t, 2H, ^3J = 7.2 Hz), 1.94−1.85 (m, 2H), 1.69−1.60 (m, 2H), 1.58−1.48 (m, 2H) ppm. ^{13}C NMR (101 MHz, DMSO-d_6): δ 194.0, 187.4, 174.3, 169.4, 157.3, 156.8, 155.0, 140.8, 128.8, 125.5, 111.3, 70.3, 33.6, 27.9, 24.9, 24.1 ppm. MS (ESI$^+$): m/z 556 $[M]^+$.

*[RuCl$_2$(Cpp-L-PNA)(CO)$_2$] (**16**).* Cpp-L-PNA (**9**) (0.250 g, 0.361 mmol) was suspended in deoxygenated methanol (15 mL) and heated to 60 °C for 15 min to complete dissolution. $[RuCl_2(CO)_2]_n$ (0.070 g, 0.307 mmol) was added, and the reaction mixture was refluxed under nitrogen for 3 h. The reaction mixture was partially concentrated (4 mL), and ether was added slowly until the solution became cloudy. The solution was cooled to −10 °C overnight to afford a yellow precipitate, which was collected by filtration, washed with ether, and dried in vacuo to obtain **16**. Yield: 0.250 g (0.270 mmol, 90%). Anal. Calcd for $C_{41}H_{44}Cl_2N_6O_8Ru$ (M_r = 920.80): C, 53.48; H, 4.82; N, 9.13. Found: C, 53.26; H, 4.94; N, 9.17. IR (KBr): ν 3419 (C−H_{arom}), 2924 (C−H_{aliph}), 2854 (C−H_{aliph}), 2066 (C≡O), 2005 (C≡O), 1702 (C═O), 1638, 1460, 1247, 1152, 1016, 756 cm^{-1}. ^1H NMR (300 MHz, CD_3CN): mixture of rotamers δ 9.54−9.50 (m, 1H), 9.20−9.17 (m, 1H), 9.03−8.94 (m, 1H), 8.42−8.20 (m, 3H), 7.91−7.74 (m, 3H), 7.65−7.59 (m, 2H), 7.39−7.29 (m, 4H), 4.36−4.31 (m, 2H), 4.23−4.18 (m, 1H), 3.97−3.86 (m, 2H), 3.48−3.38 (m, 4H), 3.30−3.19 (m, 2H), 2.40−2.20 (m, 2H), 1.64−1.60 (m, 4H), 1.44−1.38 (m, 11H) ppm. ^{13}C NMR (75 MHz, CD_3CN): mixture of rotamers δ 196.2, 196.0, 174.3, 173.5, 169.8 (maj) and 169.7 (min), 162.6 (min) and 162.5 (maj), 162.3 (min) and 162.2 (maj), 160.9 (min) and 160.8 (maj), 159.4 (min) and 159.2 (maj), 156.7, 153.6 (min) and 153.5 (maj), 152.7 (min) and 152.6 (maj), 144.5 (maj) and 144.4 (min), 141.4, 141.1 (min) and 141.0 (maj), 130.2 (min) and 130.1 (maj), 128.0 (maj) and 127.9 (min), 127.4, 127.3, 125.5 (min) and 125.4 (maj), 120.5, 120.4 (maj) and 120.3 (min), 82.3(min) and 81.4 (maj), 66.4 (maj) and 66.2 (min), 49.0, 48.6, 47.5 (min) and 47.4 (maj), 39.7 (maj) and 39.6 (min), 32.7, 32.3, 29.1 (min) and 29.0 (maj), 27.6 (maj) and 27.5 (min), 26.6 (min) and 26.5 (maj), 24.8 (maj) and 24.7 (min) ppm. MS (ESI$^+$): m/z 943.2 $[M + Na]^+$.

CO-Release Studies. The myoglobin assay was used to study CO release from the ruthenium compounds. In the assay, conversion from deoxy-myoglobin (deoxy-Mb) to carbonmonoxy-myoglobin (MbCO) is monitored spectroscopically.[80,81] The amount of CO liberated is quantified by measuring the absorbance of the MbCO Q band at 540 nm and then fitting this data with a proper function using Origin, from which the amount of CO equivalents released per mole of metal complex and the half-life can be calculated. All experiments were carried out in triplicate. For a typical measurement, a few crystals of myoglobin were dissolved in a few hundred microliters of 0.1 M phosphate buffer (PBS, pH = 7.3), placed in a quartz cuvette, and degassed with dinitrogen. Subsequently, an excess of sodium dithionite was added to convert Mb to deoxy-Mb and the concentration of

dx.doi.org/10.1021/ic400746n | Inorg. Chem. 2013, 52, 9297−9308

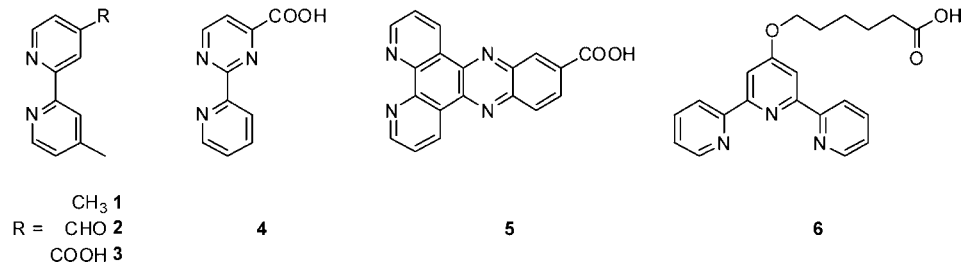

Figure 1. Polypyridyl ligands used in this study.

Scheme 1. Coupling of CppH (4) to the PNA Backbone[a]

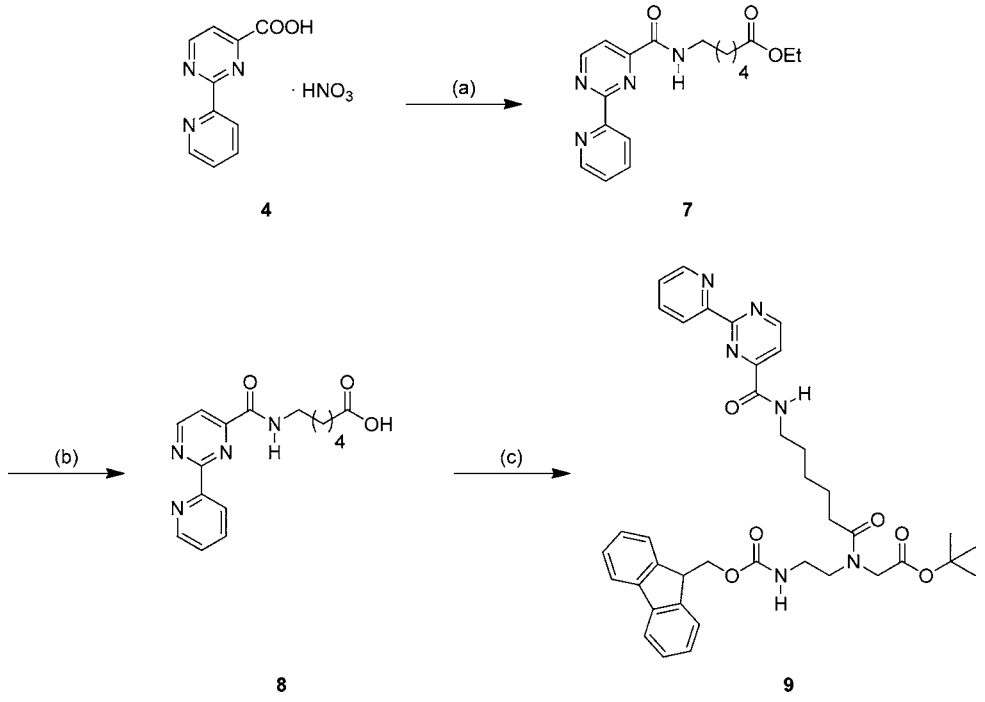

[a]Reaction and conditions: (a) ethyl 6-aminohexanoate hydrochloride, HOBt, DCC, DMAP, Et_3N, dry CH_3CN, rt, 16 h, 79%; (b) NaOH, MeOH/H_2O (3:1), 0 °C to rt, 16 h, 87%; (c) *tert*-butyl-*N*-[2-(*N*-9-fluorenylmethoxycarbonyl)aminoethyl]glycinate hydrochloride, HBTU, DMAP, dry DMF, DIPEA, rt, 18 h, 82%.

deoxy-Mb determined spectrophotometrically at 560 nm using an extinction coefficient of 13 800 L mol^{-1} cm^{-1}.[82] Spectra of this solution before and after addition of sodium dithionite were recorded to confirm complete reduction of the myoglobin. Due to the insolubility of the carbonyl complexes in aqueous buffer, approximately 3 mM stock solutions were prepared in dimethyl sulfoxide. An aliquot of the metal complex stock solution (10 μL) and PBS buffer were then added to the myoglobin solution to a total volume of 1000 μL and final concentrations of 30 μM of complex, 70 μM of myoglobin, and 10 mM dithionite while keeping $A_{557nm} < 1$. The cuvette was sealed with a plug to prevent escape of CO or reoxidation of the myoglobin. Solutions were initially kept in the dark to study the stability of the complexes in aqueous buffer and then illuminated at 365 nm using a UV hand lamp (Uvitec LF-206.LS, 6 W) until no further spectral changes could be observed for a couple of consecutive measurements. Illuminations were interrupted in regular intervals to record UV−vis absorption spectra on an Agilent 8453 UV−vis diode-array spectrophotometer. Dark control experiments were performed under the same conditions with UV−vis absorption spectra recorded automatically at regular intervals.

Ferrioxalate Actinometry. Photolytic decomposition and reduction of potassium ferrioxalate trihydrate to iron(II) was used to determine the photoflow of the light source used.[83−86] All work was carried out under very dim red light to avoid decomposition of the solutions. Thus, 147.5 mg of freshly recrystallized potassium tris(oxalato)ferrate(III) trihydrate (Strem 19−5000) was dissolved in 40 mL of deionized water, then 5 mL of 0.05 M sulfuric acid was added, and further 5 mL of deionized water was added to a total volume of 50 mL (solution A). Separately, 50 mg of anhydrous 1,10-phenanthroline (Strem 07−1650) was dissolved in 50 mL of deionized water (solution B). Finally, 3.4 g of sodium acetate trihydrate was dissolved in 25 mL of deionized water and 15 mL of this stock solution mixed with 9 mL of 0.5 M sulfuric acid and then deionized water added to a total of 25 mL (solution C). Then, the UV−vis absorption spectrum of a freshly prepared 0.006 M solution A was measured to check for zero absorption at 510 nm to ensure that no decomposition had occurred so far. For the measurements, 3 mL of a 0.006 M solution A were pipetted into a cuvette and illuminated at 365 nm using a UV hand lamp (Uvitec LF-206.LS, 6 W) with stirring for a given time determined with a digital stopwatch. Then, 1 mL thereof was transferred to a 10 mL volumetric flask containing 1 mL of solution B and 0.5 mL of buffer C. Deionized water was added to a total of 10 mL. In addition, 1 mL of nonilluminated solution A was treated in exactly the same way, and both solutions were stored in absolute darkness for at least 1 h. Their absorptions were determined at 510 nm on an Agilent 8453 spectrophotometer, and the concentration of $[Fe(phen)_3]^{2+}$ was calculated using a molar extinction coefficient of ε_{510nm} = 11 100 L mol^{-1} cm^{-1}.[86] The experiment was

dx.doi.org/10.1021/ic400746n | *Inorg. Chem.* 2013, 52, 9297−9308

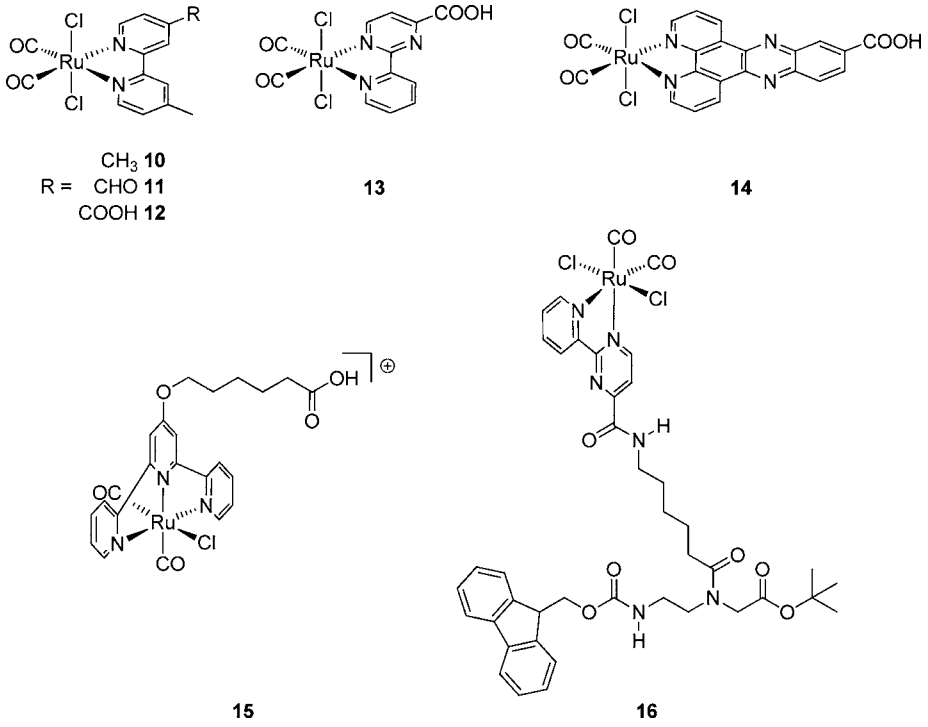

Figure 2. Series of ruthenium(II) carbonyl complexes **10**–**16** synthesized in this work.

repeated for at least five different illumination times, and absorbance was plotted against time to ensure that no complete bleaching of the actinometer solution occurred. Otherwise, the illumination time has to be decreased accordingly. Then, the amount of iron(II) ions formed at a given illumination interval was calculated according to

$$n(Fe^{2+}) = V_1 \cdot V_3 \cdot \Delta A(510\text{nm})/(10^3 \cdot V_3 \cdot l \times \varepsilon(510\text{nm})) \quad (1)$$

in which V_1 is the volume of the illuminated ferrioxalate solution, V_2 is the aliquot thereof taken for determination of ferrous iron, and V_3 is the final volume after complexation with phenanthronline (all in milliliters). $\Delta A(510\text{ nm})$ is the difference in absorption between the illuminated solution and the nonilluminated control, l the path length of the cuvette in cm, and $\varepsilon_{510\text{ nm}}$ the molar extinction coefficient of $[Fe(phen)_3]^{2+}$. The photon flow ϕ_P passing through the cuvette per second is then calculated as

$$\phi_p = n(Fe^{2+})/(t \times \phi_\lambda) \quad (2)$$

where $n(Fe^{2+})$ is the molar amount of ferrous iron produced during the illumination time t and ϕ_λ is the quantum yield for production of iron(II) at the illumination wavelength used taken from the literature. Here, a value of $\phi_\lambda = 1.21$ was used for the excitation wavelength of 365 nm.[83−85] Under the conditions described above, a quantum flow of about 2.4×10^{-8} Einstein s^{-1} was determined for our setup and remained relatively stable over repeated determinations, with fluctuations in quantum flow from day to day estimated to be in a range of a maximum of about ±20%.

RESULTS AND DISCUSSION

Ligand Synthesis. Polypyridyl ligands $bpy^{CH3,CH3}$ (**1**),[68] $bpy^{CH3,CHO}$ (**2**),[69] $bpy^{CH3,COOH}$ (**3**),[69] CppH (**4**),[70] dppzcH (**5**),[71] and tpy^{COOH} (**6**),[67] which are shown in Figure 1, were synthesized according to literature procedures.

The modified PNA monomer, Cpp-L-PNA (**9**), was prepared according to the procedure outline in Scheme 1. Briefly, the carboxamido derivative **7** was obtained by HOBt/DCC-mediated coupling of the free carboxylic acid group in **4** and the amino group in ethyl 6-aminohexanoate. Hydrolysis with base yielded the carboxylic acid derivative **8**. Successful formation of **8** is demonstrated by the disappearance of a distinct quartet at 4.12 ppm ($-OCH_2CH_3$) and a triplet at 1.24 ppm ($-OCH_2CH_3$) of the ethyl ester group found in the ^1H NMR spectrum of **7**. The IR spectrum of **7** shows two CO stretching vibrations at 1670 and 1730 cm^{-1}, as expected for an amide and ester functionality. These signals were slightly shifted in the carboxylic acid **8** to 1679 and 1697 cm^{-1}, respectively. The ESI-MS exhibited peaks at m/z = 315.2 and 337.1 which can be assigned to $[M + H]^+$ and $[M + Na]^+$, respectively. Due to its poor stability in the neutral form, the PNA monomer backbone was prepared and stored as its hydrochloride salt using the method described by Thomson et al.[72] The modified PNA monomer Cpp-L-PNA (**9**) was obtained by classical amide coupling between the secondary amine on the monomer backbone and the free carboxylic acid group present in **8**. The PNA monomer backbone was neutralized in situ by addition of diisopropylamine at 0 °C to prevent cleavage of the base-labile Fmoc protecting group, thereby resulting in a 3-fold improvement in yield. The final product Cpp-L-PNA (**9**) was obtained in 82% yield after chromatographic purification. The ^1H NMR spectrum of Cpp-L-PNA (**9**) exhibits the expected signals due to the Fmoc and the *tert*-butyl group in addition to resonances similar to those found for **8**. The IR spectrum shows three CO stretching vibrations at 1648, 1650, and 1703 cm^{-1} due to one ester and two amide functionalities as well as N−H (3328−3337 cm^{-1}), aromatic C−H (3008−3082 cm^{-1}), and aliphatic C−H (2856−2985 cm^{-1}) stretches. The ESI-MS shows one peak at m/z = 715.3 corresponding to the $[M + Na]^+$ ion, providing further confirmation for formation of **9**.

Complex Synthesis.[72,73] A series of ruthenium(II) complexes (Figure 2) was prepared by reaction of the key synthon $[RuCl_2(CO)_2]_n$ with the respective bi- or tridentate ligands under an inert atmosphere. Since it was reported that some Ru(II)−2,2′-bipyridine complexes undergo ultrafast CO release in solution upon illumination,[65,66] all preparations were

dx.doi.org/10.1021/ic400746n | Inorg. Chem. 2013, 52, 9297−9308

performed under strict exclusion of light. Three complexes with 4-substituted 2,2′-bipyridine ligands were prepared in order to investigate the influence of functional groups attached to the π system of the bpy on the CO-release behavior and also to act as a potential anchor for the synthesis of bioconjugates. Preparation of $[RuCl_2(bpy^{CH3,CH3})(CO)_2]$ (**10**) was first reported by Strouse et al.,[78] who described the reaction of $[RuCl_2(CO)_2]_n$ with $bpy^{CH3,CH3}$ (**1**) in methanol at reflux, which resulted in precipitation of **10** as yellow needles. We performed this reaction in a microwave reactor, thereby reducing the reaction time from 15 to 2 min, but the yield of 50% was not improved using this method. Use of a similar microwave-assisted procedure in the reaction of $[RuCl_2(CO)_2]_n$ with $bpy^{CH3,CHO}$ (**2**) did not lead to precipitation of the desired product $[RuCl_2(bpy^{CH3,CHO})(CO)_2]$ (**11**). In contrast, upon cooling, cubic yellow crystals suitable for X-ray crystal structure analysis were obtained, which unexpectedly revealed them to be those of the hemiacetal complex $[RuCl_2(bpy^{CH3,CH(OH)(OCH3)})(CO)_2]$ with a *cis*-dicarbonyl arrangement in the ligand sphere of the octahedral ruthenium center (see Supporting Information Figure S1). Further cooling resulted in coprecipitation of **11** and the hemiacetal complex as yellow needles. Synthesis was therefore repeated in tetrahydrofuran to avoid acetal formation of $bpy^{CH3,CHO}$ with the alcoholic solvent, and in this case, the crude product precipitated without additional cooling. After chromatographic purification in the dark, **11** was obtained in excellent purity but a rather low yield of 25%. $[RuCl_2(bpy^{CH3,COOH})(CO)_2]$ (**12**) was synthesized following the procedure of Spiccia and co-workers.[75] Similar reaction conditions were employed for preparation of $[RuCl_2(CppH)(CO)_2]$ (**13**), $[RuCl_2(dppzcH)(CO)_2]$ (**14**), and $[RuCl_2(Cpp\text{-}L\text{-}PNA)(CO)_2]$ (**16**). $[RuCl_2(CO)_2]_n$ was added to a methanolic solution of **4**, **5**, and **9**, respectively, and heated to reflux in the dark. Subsequent cooling of the reaction mixtures overnight ensured complete precipitation of the desired complexes **13** and **14** in good yield (60−85%).

Reaction of $[RuCl_2(CO)_2]_n$ with tpy^{COOH} (**6**) in a water/ethanol mixture afforded the monocationic complex $[RuCl(CO)_2(tpy^{COOH})]^+$ (**15**), which was precipitated with ammonium hexafluorophosphate and recrystallized to give an isolated yield of 47%. In the case of the Cpp-L-PNA complex **16**, concentration of the reaction mixture, layering with diethyl ether, and cooling overnight afforded the product in 90% yield. ESI-MS and elemental analysis confirmed successful synthesis of all target compounds. In addition, the ligand coordination mode was also established by comparison of the ^{1}H NMR spectra of the free ligand and complexes. ^{1}H NMR spectra of complexes **10**−**12** show an upfield shift of the aromatic protons, whereas for complex **15**, the aromatic protons are shifted downfield by about 0.5 ppm. All ruthenium(II) complexes prepared show two strong C≡O stretching vibrations between 1986 and 2013 and 2057−2076 cm^{-1}, with the higher energy one assigned to the symmetrical and the lower energy one to the asymmetrical $Ru(CO)_2$ stretching vibration, as also reported for $[RuCl_2(bpy)(CO)_2]$, Table 1.[74] Furthermore, C═O stretching vibrations for the aldehyde and carboxylic acid groups appear at 1702 and 1744 cm^{-1}. For the Cpp-L-PNA ruthenium(II) complex, a vibration at 1638 cm^{-1} is ascribed to the amide group.

UV−Vis Absorption Spectroscopy. UV−vis absorption spectra of complexes **10**, **12**, and **13** as well as **14**−**16** in dimethyl sulfoxide and acetonitrile solution are shown in Figures 3 and 4, respectively. Extinction coefficients were determined at the excitation wavelength of 365 nm as well as the most prominent absorption maxima and are summarized in Table 2. As is typically the case for Ru(II) polypyridyl complexes, spectra are dominated by MLCT (metal-to-ligand charge transfer) transitions from d orbitals of the ruthenium(II) center to multiple low-lying ligand π^* levels. The prototype of these compounds is $[Ru(bpy)_3]^{2+}$, which has absorption maxima at 240, 285, and 450 nm,[59] with the band at 285 nm assigned to the LC transitions and the remaining two bands to MLCT transitions.[59] Similar absorption maxima have also been reported for carbonyl compounds related to compounds **10**−**16**.[63,87] For the bipyridine and terpyridine Ru(II) complexes

Table 1. Comparison of Carbonyl Vibrational Bands of Complexes 10−16 with Those of $[RuCl_2(bpy)(CO)_2]$[74]

complex	sym(C≡O) [cm^{-1}]	asym(C≡O) [cm^{-1}]	C═O [cm^{-1}]	C(═O)NR [cm^{-1}]
$[RuCl_2(bpy)(CO)_2]$	2057	1998		
10	2058	1986		
11	2058	1991	1704	
12	2072	2012	1720	
13	2068	2006	1744	
14	2068	2007	1718	
15	2076	2013	1704	
16	2066	2005	1702	1638

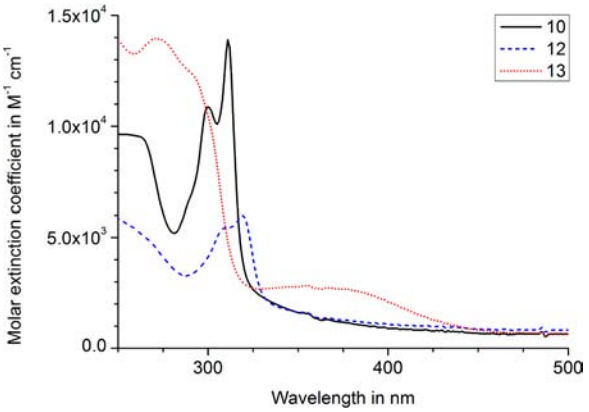

Figure 3. UV−vis absorption spectra of **10** (65 μM) and **12** (61 μM) in dimethyl sulfoxide and **13** (74 μM) in acetonitrile.

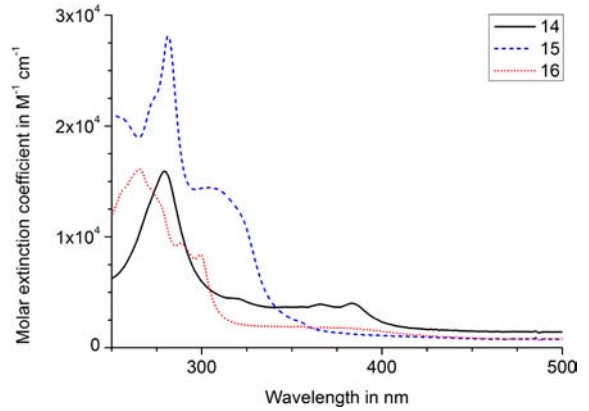

Figure 4. UV−vis absorption spectra of **14** (65 μM) and **16** (62 μM) in acetonitrile and **15** (56 μM) in dimethyl sulfoxide.

dx.doi.org/10.1021/ic400746n | Inorg. Chem. 2013, 52, 9297−9308

Table 2. Spectroscopic Data of the Ruthenium(II) Complexes[a]

complex	λ_{max} [nm]	ε_{λ} [M^{-1} cm^{-1}]	$\varepsilon_{365\ nm}$ [M^{-1} cm^{-1}]
10[b]	301, 311	10 100 ± 560, 12 575 ± 800	1560 ± 100
11	n.d.	n.d.	n.d.
12[b]	311, 319	8690 ± 310, 9740 ± 360	1135 ± 75
13[c]	271, 326	13 900 ± 95, 2360 ± 110	2450 ± 80
14[c]	281, 317	15 120 ± 760, 4420 ± 220	3890 ± 190
15[b]	291, 303	30 020 ± 680, 15 575 ± 210	1380 ± 100
16[c]	265, 289, 299	25 910 ± 200, 15 025 ± 170, 13 460 ± 160	2540 ± 165

[a]n.d. not determined. [b]In DMSO solution. [c]In acetonitrile solution.

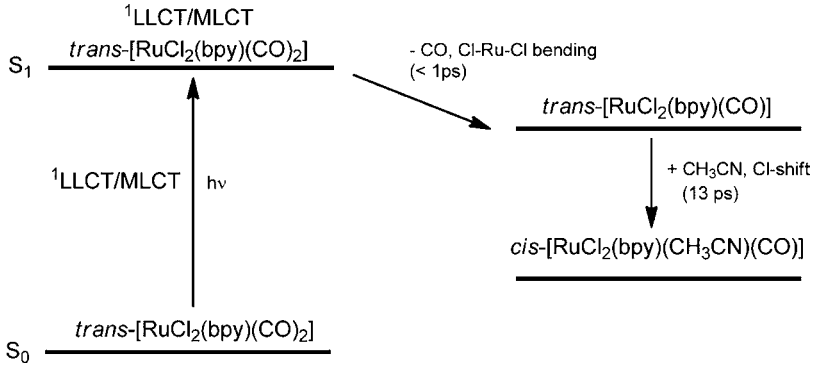

Figure 5. Proposed mechanism for photochemical CO substitution in ruthenium dicarbonyl complexes.[89]

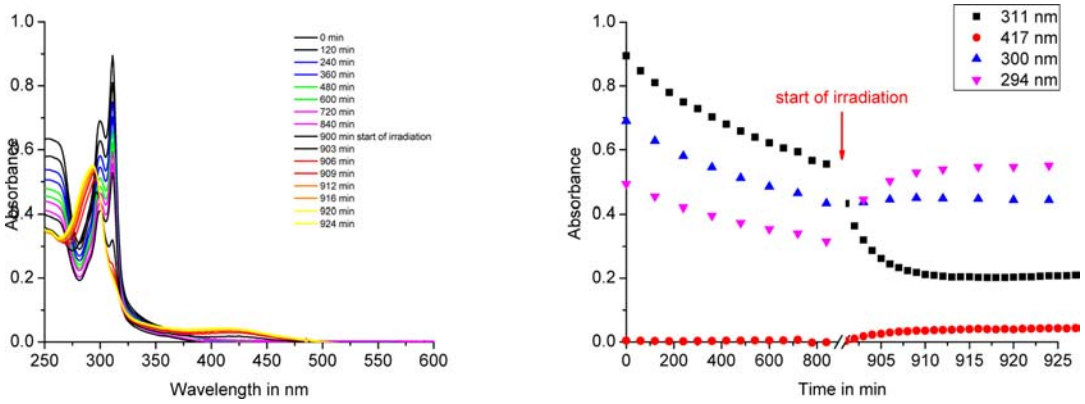

Figure 6. Spectral changes occurring during the dark incubation of a 60 μM solution of complex **10** in water/dimethyl sulfoxide (98:2 v/v) over 15 h and subsequent illumination at 365 nm for up to 25 min.

reported herein, two main absorption bands are observed, one below and one above 300 nm, although the intensity ratio is reversed for bipyridine compared to terpyridine. From the spectra of **10** and **12**, it can be concluded that transitions to the lowest π^* level of each ligand are influenced by the substituents on the bipyridine ligand. Replacement of the electron-donating bpy^{CH3,CH3} ligand by an electron-withdrawing bpy^{CH3,COOH} one (**10** → **12**) results in a decrease of the absorption intensity together with a bathochromic shift (see Table 2). This indicates that the $\pi \rightarrow \pi^*$ energy gap is reduced.

For the CppH complex **13** and the dppzcH complex **14**, changes in the π system of the ligand or its extension cause a significant change in the absorption spectra. For **13**, new LC transitions appear in the near-UV region (250−300 nm)[70] together with a weak but significant plateau at around 375 nm. In contrast, extension of the π system as in **14** leads to one strong LC band at 281 nm and two bathochromically shifted weak bands at 350−380 nm. As previously observed for dppzcH-containing complexes, these two bands may be attributed to the intraligand ($\pi \rightarrow \pi^*$) transitions in dppzcH.[71] Complex **15** shows a hypsochromic shift for the two peaks at around 300 nm when compared to the bipyridine-based counterparts (see Table 2), which may be due to the lower symmetry of the molecule. In addition to the hypsochromic shift of the absorption bands, when compared to the reported monocarbonyl terpyridine complex, *trans*-[RuCl$_2$(CO)(tpy)], compound **15** exhibits $\pi \rightarrow \pi^*$-based transition rather than a MLCT transition due to the presence of an additional carbonyl ligand. UV−vis absorption spectra of Ru(II)−Cpp-L-PNA complex **16** show an absorption band distribution quite similar to complex **13**. It exhibits characteristic absorption peak maxima for the corresponding LC transition in the spectral region below 300 nm as well as a weak absorption band at around 370 nm.

Preliminary stability and photolysis experiments were also carried out on **10** and **12**−**16** to check for the stability of the compounds in solution in the dark as well as their potential photolability, in particular, of the carbonyl ligand(s). Photolysis

dx.doi.org/10.1021/ic400746n | Inorg. Chem. 2013, 52, 9297−9308

of $[RuCl_2(L)(CO)_2]$ complexes (L = bpy, 4,4′-dicarboxy-bpy, 4,4′-di(isopropoxycarbonyl)-bpy) has been reported previously, resulting in replacement of the CO ligands by solvent molecules.[63,88] Additionally, a mechanism for this substitution was proposed with the aid of time-resolved IR spectroscopy and DFT calculations.[65] Gabrielsson et al. suggested that the ruthenium(II) complex is excited to a singlet state which then undergoes very fast CO release. Subsequently, the solvent molecule, which was acetonitrile in the reported case, binds to the five-coordinated intermediate to give the *cis*(Cl,Cl)-isomer of the acetonitrile complex (Figure 5).

In order to investigate the stability and photochemical behavior, water/dimethyl sulfoxide (98:2 v/v) solutions of our complexes were first incubated in the dark for up to 24 h and then exposed to the light of a 6 W UV hand lamp at 365 nm. During dark incubation, UV−vis absorption spectra were automatically recorded at regular intervals while illumination was interrupted at fixed times to collect absorption spectra. Although the excitation wavelength of 365 nm does not match with the band maxima of the compounds, all of them still show sufficient absorption at this wavelength with molar extinction coefficients of about 1100−3900 M^{-1} cm^{-1} (Table 2).

Compound **10** is not stable under these conditions in the dark. The intensity of the two bands at 301 and 311 nm decreases with incubation time without reaching a final plateau level even after 15 h. The loss of intensity is more pronounced for the latter band, and no new signals appear. The same solution was then illuminated at 365 nm, and UV−vis absorption spectra were recorded at 1 min intervals (Figure 6). The intensity of the 311 nm band decreases further, but at a much faster rate, and finally reaches a plateau level after about 20 min of illumination. At 301 nm, the loss of intensity does not continue and instead the absorption at that wavelength slightly increases again with illumination time. In addition, two new bands grow in at 294 and 417 nm and reach saturation on a similar time scale. The red shift of the latter band is consistent with those previously reported for similar ruthenium(II) carbonyl compounds undergoing photochemical carbonyl substitution.[62,63,88]

Complex **12**, with the $bpy^{CH3,COOH}$ instead of the $bpy^{CH3,CH3}$ ligand as in **10**, on the other hand, does not show any noticeable change in the absorption spectrum, in particular, of the two main bands at 311 and 319 nm, upon incubation in water/dimethyl sulfoxide (98:2 v/v) for up to 23 h (Figure S2, Supporting Information). When this solution is then photoexcited at 365 nm, however, these two bands quickly disappear and two new signals grow in with maxima at 302 and 426 nm, reaching saturation on a similar time scale (data not shown).

The same is also true for compound **13**, which is stable under the same conditions as mentioned above when kept in the dark for up to 21 h (Figure S3, Supporting Information). However, when this is followed by illumination at 365 nm, there is a slight bathochromic shift in the high-energy absorption maximum from about 270 to 285 nm while the red edge of this band shifts to high energies by about 5 nm. The absorption at around 350 nm remains essentially the same throughout the experiment, but an additional quite intense absorption grows in at longer wavelengths during photoexcitation, with two maxima at 401 and 504 nm. These reach saturation after about 15 min of illumination time.

The dppzcH complex **14** is also stable in the dark in aqueous solution for up to 23 h (Figure S4, Supporting Information). Illumination at 365 nm leaves the major peaks at 281 nm and in the region from about 340 to 385 nm more or less unchanged, although the latter set of signals experiences a slight shift to higher energies by a few nanometers with the overall intensity essentially unaltered. The major new feature that appears upon photoexcitation is a broad band between 420 and 600 nm with a maximum at 473 nm, which, however, does not fully reach saturation after 20 min of illumination time.

The tpy compound **15** shows two major peaks at 291 and 303 nm, which are only marginally shifted upon incubation in the dark for up to 23 h, and thus, this complex is also to be considered dark stable (Figure S5, Supporting Information). The following photoexcitation at 365 nm, however, leads to pronounced spectral changes. The 291 and 303 nm peaks gradually decrease in intensity, and new peaks grow in with a maximum at 272 nm and a shoulder at around 295 nm. In addition, two new very broad peaks appear in the low-energy part of the spectrum between 350 and 500 nm, with maxima centered at 363 and around 445 nm. The behavior of the PNA conjugate **16** is very similar to that of the parent compound **13**. The intense bands at 265, 289, and 299 nm remain essentially unchanged in position and intensity throughout the experiment, regardless of dark incubation or photoexcitation, with only the latter marginally gaining in intensity (Figure S6, Supporting Information). However, more pronounced changes can be observed in the visible region of the spectrum upon illumination at 365 nm. A very broad absorption grows in between 350 and 600 nm with peaks centered at 389 and 495 nm.

In summary, with the exception of $[RuCl_2(bpy^{CH3,CH3})(CO)_2]$, **10**, the other complexes **12**−**16** are stable in aqueous solution for up to 24 h under exclusion of light and, thus, suitable candidates for further evaluation as PhotoCORMs. Upon photoexcitation at 365 nm, however, all compounds show pronounced changes in their UV−vis absorption spectra with a very broad new absorption growing in between 400 and 600 nm. In addition, the bpy and tpy compounds also experience significant changes in the range of 250−350 nm, whereas this region of the spectrum remains essentially constant for the Cpp and dppz complexes. In order to check whether the changes observed in the absorption are indeed due to a photoinduced release of carbon monoxide from the metal coordination sphere and to see whether only one or both CO ligands are liberated, the myoglobin assay was applied.

CO-Release Studies. The standard method to investigate the CO-release behavior of metal carbonyl complexes under physiological conditions is the myoglobin assay, which takes advantage of the different absorptions of deoxy-Mb and carboxy-Mb.[80,81] Deoxy-Mb shows a characteristic absorption maximum in the Q-band region at 557 nm, while carboxy-Mb (MbCO) has two absorption maxima centered at 540 and 577 nm.[82] Thus, CO release from metal complexes and transfer to Mb can be monitored spectrophotometrically. The reaction conditions for this study were chosen to ensure that at least a 2-fold excess of myoglobin over complex was maintained all the time to provide one Mb for each carbonyl that can potentially be released from the metal coordination sphere. To investigate the stability of the Ru(II) complexes under physiological conditions in the dark, mixed solutions of PhotoCORMs and myoglobin were carefully protected from light and their UV−vis absorption spectra recorded in regular intervals.

All compounds **10** and **12**−**16** studied showed negligible spectral changes over 60 min of incubation in the dark and can thus be considered as stable and inactive toward CO release

dx.doi.org/10.1021/ic400746n | *Inorg. Chem.* 2013, 52, 9297−9308

under the conditions of the myoglobin assay (Figure 7). Upon extended incubation for up to 15 h in the dark, **10**, **12**, and **13**

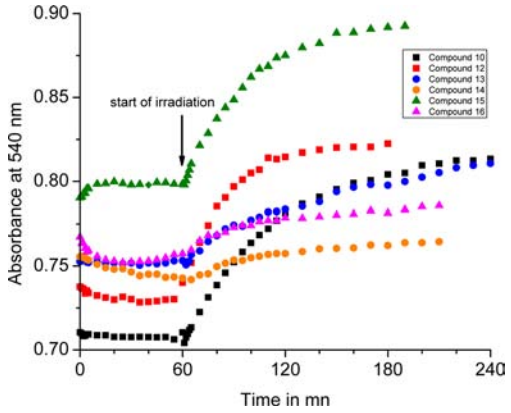

Figure 7. Formation of MbCO in mixtures of compounds **10** and **12**–**16** with reduced myoglobin was followed by monitoring changes in the absorption at 540 nm. Illumination was started after 60 min. Initial constant absorptions indicate the stability of the compounds in the dark.

were also stable and showed no signs of carbon monoxide release. However, for **15** and **16**, spectral changes in the 540–577 nm range were observed which indicate at least some minor degree of decomposition and CO release on this time scale (data not shown).

Subsequently, fresh solutions of the complexes mixed with reduced myoglobin were preincubated for 1 h in the dark and then illuminated at 365 nm. Spectral changes in the Q-band region of Mb were observed for all compounds, indicating that CO is released from the metal complexes but to a different degree and at a different rate. Plateau values with no more MbCO formed even upon prolonged photoexcitation were reached for all compounds after about 3 h of illumination.

To determine the number of CO equivalents released per mole of ruthenium(II) complex, the concentration of MbCO after extended illumination was calculated utilizing eq 3, which is derived from the Lambert–Beer law under the assumption that the total concentration of Mb species is constant throughout the assay (see Supporting Information). Thus, at a particular time t, the concentration of MbCO can be expressed in terms of the initial concentration of myoglobin c_0(Mb), the path length of the cuvette l, the absorption at $t = 0$, and the molar extinction coefficient of Mb at 540 nm, the latter taken from the literature as $\varepsilon_{540nm} = 15.4\ mM^{-1}\ cm^{-1}$.[82]

$$c(\mathrm{MbCO}) = \left(\frac{A(t)}{l} - \frac{A(t=0)}{l}\right) \frac{1}{\varepsilon_{540nm}(\mathrm{MbCO}) - \frac{A(t=0)}{c_0(\mathrm{Mb})\cdot l}} \quad (3)$$

The calculated MbCO concentration was plotted against the illumination time as shown for **10** in Figure 8. By applying a suitable fit function, the plateau level of the MbCO concentration was determined and subsequent division by the complex concentration gave the number of CO equivalents released per mole of complex. Furthermore, the rate constant and corresponding half-life for CO release under these conditions can also be obtained from the fit. All measurements

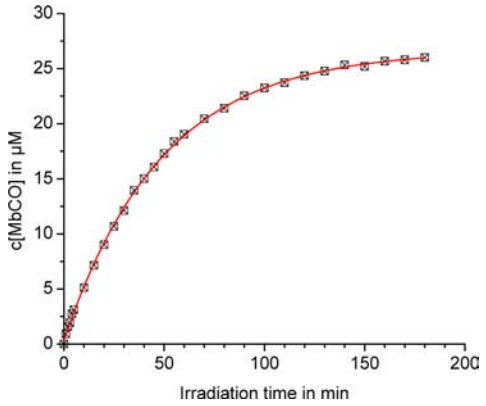

Figure 8. Time-dependent formation of MbCO upon illumination at 365 nm of a mixture of **10** (30 μM) and myoglobin (70 μM) in 0.1 M PBS buffer.

were performed at least in triplicate, and the mean values resulting from these calculations are summarized in Table 3.

Table 3. Number of CO Equivalents Liberated Per Mole of Metal Complex upon Photoexcitation at 365 nm and Half-Life for CO Release[a]

complex	equivalents of CO	$t_{1/2}$ [min]
10	0.9 ± 0.1	31 ± 9
11	n.d.	n.d.
12	0.7 ± 0.2	20 ± 2
13	0.5 ± 0.1	66 ± 17
14	0.2 ± 0.1	49 ± 19
15	0.6 ± 0.1	21 ± 5
16	0.3 ± 0.1	24 ± 10

[a]All determinations were carried out at least in triplicate. n.d. not determined.

The myoglobin assay shows that all ruthenium(II) complexes investigated herein liberate CO upon illumination at their respective absorption maximum. However, the half lives and number of CO equivalents released per mole of complex vary from complex to complex. For complexes **10** and **12**, one of the two carbonyl ligands is liberated from the metal coordination sphere. In contrast, although CO release from **13**–**16** is evident from the myoglobin assay, the calculated amount of carbon monoxide liberated was found to be significantly less than 1 equiv per mole of complex. In particular, CO release for **13**, **14**, and **16** was rather slow, and thus, a plateau level for MbCO formation was not reached even after a maximum illumination time of 180 min. Most importantly, no significant differences in the CO-release properties could be observed for **13** vs **16**. Thus, when the parent molecule containing the CppH ligand is attached to the PNA monomer backbone, changes in the metal coordination sphere affecting the CO-release properties are negligible. Photochemical decarbonylation of $[RuCl_2(bpy)(CO)_2]$ and $[RuCl_2(bpy^{CH3,CH3})(CO)_2]$ complexes has been studied before in coordinating solvents such as acetonitrile or pyridine. It was suggested that the initial photodissociation of one equatorial CO ligand is followed by a rearrangement of the ligand sphere and solvent coordination to form $[RuCl_2(bpy)(CO)(solvent)]$.[62,90] However, the data provides no information as to whether this might occur via a five-coordinate ruthenium species or an addition–elimination mechanism. Despite the reported very small trans-labilizing effect of 2,2′-

dx.doi.org/10.1021/ic400746n | Inorg. Chem. 2013, 52, 9297–9308

bipyridine,[91] there is a notable influence on the CO-release properties when this system is modified. A reduction of the ring electron density, e.g., by introduction of functional groups or additional ring nitrogens, affects the metal−polypyridyl ligand d−p orbital overlap.[92] We observe that this goes along with a prolonged half-life of the compounds while the released amounts of CO are more or less the same. On the other hand, the ruthenium carbonyl complex **15** with the extended, electron-rich terpyridine π system has a shorter half-life than all other compounds. Interestingly, there is no obvious correlation of the number of CO equivalents released or the half-life with the extinction coefficient of the compounds (see Table 3). For example, although **10** and **12** together with **15** have the least intense absorption at an excitation wavelength of 365 nm, they show the most efficient CO release and among the fastest release kinetics in the series, while compound **14** with the largest extinction coefficient at 365 nm is the least efficient releaser and has a much longer half-life under otherwise identical conditions in the series. The CO stretching vibrations presented in Table 4 do not seem to show any correlation with the number or time scale of the CO release reported in Table 3. It is likely that other, more subtle factors influence the rates of CO release.

Table 4. Quantum Yield of CO Released under the Conditions of the Myoglobin Assay[a]

complex	quantum yield
10	$(2.3 \pm 1.2) \times 10^{-4}$
11	n.d.
12	$(4.6 \pm 1.0) \times 10^{-4}$
13	$(1.4 \pm 0.2) \times 10^{-4}$
14	$(5.0 \pm 0.3) \times 10^{-5}$
15	$(3.7 \pm 0.1) \times 10^{-4}$
16	$(1.8 \pm 0.2) \times 10^{-4}$

[a]All determinations were carried out at least in triplicate. n.d. not determined.

Furthermore, the quantum yield of CO release was determined with the aid of ferrioxalate actinometry under the conditions of the myoglobin assay. The very low quantum yields reported in Table 4 are due to the presence of the myoglobin in the solution, which has a non-negligible absorption at an excitation wavelength of 365 nm, leading to an internal shielding effect in which only part of the total photon flux is available for CO photorelease. Since the myoglobin concentration is kept constant in all these experiments, at 70 μM, as mentioned in the Experimental Section, the inner shielding effect from the Mb absorption is the same for all compounds tested and thus the values are comparable. Therefore, a correction for the internal filtering was not made to obtain the absolute values. The quantum yield data are not absolute values and only reflect the relative ratio of the determined quantum yields. Nevertheless, we consider these as the most realistic conditions when having potential biological applications in mind, since cellular environments will also provide significant amounts of heme proteins with absorption in this range. The data shows that the bipyridine and terpyridine compounds, **10**, **12**, and **15**, show a slightly more efficient CO release compared to the CppH and dppzcH complexes, **13**, **14**, and **16**, as indicated by the somewhat higher quantum yields, but the differences are not very large. Interestingly, there is also no direct correlation between quantum yield and absorption intensity at an excitation wavelength of 365 nm, since compounds **10**, **12**, and **15** with the highest quantum yields actually have the lowest ε_{365nm} values in the series (see Table 2). This suggests that more subtle differences in the electronic structure of these compounds determine the efficiency of the CO-release process.

In particular, the bpy and tpy complexes, **10**, **12**, and **15**, show promising PhotoCORM behavior with relatively short half-lives of CO release. However, the excitation wavelength of 365 nm will require a further tuning of the photophysical and photochemical properties to ensure deep tissue penetration and minimize photodamage of tissue which has not accumulated the metal carbonyl complexes.[57,58]It is expected that the rich chemistry of ruthenium polypyridyl compounds will allow us to achieve these goals, for example, via modifications on the chelating ligand backbone as, for example, replacement of bpy by a η^2-coordinating tpy or introduction of a second additional ligand with π systems.[93]

CONCLUSIONS

In this work, a series of ruthenium(II) dicarbonyl complexes with functionalized 2,2′-bipyridine, 2,2′:6′,2″-terpyridine, 2-(pyridin-2-yl)pyrimidine, and dipyrido[3,2-a:2′,3′-c]phenazine ligands has been synthesized as well as a novel PNA-like monomer containing the 2-(pyridin-2-yl)pyrimidine ligand. The bidentate chelating site available on the 2-(pyridin-2-yl)pyrimidine ligand makes this PNA-like monomer a useful template for preparation of novel metal−PNA bioconjugates, where the metal complex can be introduced at the location of interest within the PNA oligomer via post- and preoligomer synthesis. Interest in such metal-containing PNA−bioconjugates derives from numerous biosensing and biomedical applications.[94] However, here we focused mainly on understanding the CO-release properties of the corresponding Ru(II) dicarbonyl complexes which might be suitable as novel PhotoCORMs. As such, complex $[RuCl_2(Cpp\text{-}L\text{-}PNA)(CO)_2]$ was prepared, which to the best of our knowledge is the first successful incorporation of a Ru(II) dicarbonyl unit onto a PNA monomer backbone. The myoglobin assay was used to study the photoinduced CO release for all ruthenium complexes prepared, which showed all of them to be stable under physiological conditions in the dark for up to 1 h and most even for an extended period time of 15 h, but release CO upon illumination at 365 nm, in the low-energy shoulder of their main absorption peak. While the two complexes carrying a substituted 2,2′-bipyridine ligand were found to release 1 equiv of CO per complex, the terpyridine, dipyrido[3,2-a:2′,3′-c]phenazine, and 2-(pyridin-2-yl)pyrimidine-based complexes liberated less than 1 mol of CO per mole of metal complex. However, attachment of the complex to the PNA backbone did not produce any significant alteration in the spectroscopic or CO-release properties of $[RuCl_2(Cpp\text{-}L\text{-}PNA)CO_2]$, indicating that the intrinsic PhotoCORM nature of the parent molecular unit can be retained when such Ru(II)−carbonyl complexes are incorporated into bioconjugates like PNA. Thus, a novel class of photoactivatable functionalized ruthenium(II)-based CORMs has been established. Future work in this direction will focus on development of complexes which release CO upon excitation at longer wavelength or using two-photon absorption to trigger the CO release and coupling of these new CO-releasing molecules to biological carriers as well as insertion into PNA oligomers and investigating their behavior on in vitro and ultimately in vivo systems.

dx.doi.org/10.1021/ic400746n | Inorg. Chem. 2013, 52, 9297−9308

■ ASSOCIATED CONTENT

Supporting Information

Synthesis of ligands **7**, **8**, and **9**; X-ray crystal structure determination of $[RuCl_2(bpy^{CH3,CH(OH)(OCH3)})(CO)_2]$; absorption spectra for the dark stability and photolysis studies for compounds **12**−**16**. This material is available free of charge via the Internet at http://pubs.acs.org.

■ AUTHOR INFORMATION

Corresponding Author

*Phone: +49 (0)931-31-83636. Fax: +49 (0)931-31-84605. E-mail: ulrich.schatzschneider@uni-wuerzburg.de.

Present Address

[§]Institut für Anorganische Chemie, Julius-Maximilians-Universität Würzburg, Am Hubland, D-97074 Würzburg, Germany.

Notes

The authors declare no competing financial interest.

■ ACKNOWLEDGMENTS

This work was supported by the Deutsche Forschungsgemeinschaft (DFG) within FOR 630 "Biological function of organometallic compounds" (U.S.) and the Australian Research Council through the Australian Centre of Excellence for Electromaterials Science (L.S.). C.B. thanks the Deutscher Akademischer Austauschdienst (DAAD) for a semester fellowship for postgraduates. T.J. was the recipient of Monash Graduate Scholarship, Monash International Postgraduate Research Scholarship and Postgraduate Publication Award. A.D. was on a summer internship at the University of Würzburg from the Indian Institute of Technology Bombay (IITB). L.S. thanks the Alexander von Humboldt Foundation for a Senior Research Award. We also thank Sandesh Pai, Mark Ehrlich, and Jennifer Weiss for their assistance with the initial CO-release measurements.

■ REFERENCES

(1) Foresti, R.; Motterlini, R. *Curr. Drug Targets* **2010**, *11*, 1595−1604.
(2) Kajimura, M.; Fukuda, R.; Bateman, R. M.; Yamamoto, T.; Suematsu, M. *Antioxid. Redox Signaling* **2010**, *13*, 157−192.
(3) Ryter, S. W.; Alam, J.; Choi, A. M. K. *Physiol. Rev.* **2006**, *86*, 583−650.
(4) Abraham, N. G.; Kappas, A. *Pharmacol. Rev.* **2008**, *60*, 79−127.
(5) Piantadosi, C. A. *Free Radical Biol. Med.* **2008**, *45*, 562−569.
(6) Vreman, H. J.; Wong, R. J.; Stevenson, D. K. Carbon Monoxide and Cardiovascular Functions. In *Carbon Monoxide and Cardiovascular Functions*; Wang, R., Ed.; CRC Press: Boca Raton, FL, 2002; pp 273−308.
(7) Kharitonov, V. G.; Sharma, V. S.; Pilz, R. B.; Magde, D.; Koesling, D. *Proc. Natl. Acad. Sci. U.S.A.* **1995**, *92*, 2568−71.
(8) Stone, J. R.; Marletta, M. A. *Biochemistry* **1995**, *34*, 16397−403.
(9) Kim, H. P.; Ryter, S. W.; Choi, A. M. K. *Annu. Rev. Pharmacol. Toxicol.* **2006**, *46*, 411−449.
(10) Hou, S.; Heinemann, S. H.; Hoshi, T. *Physiology* **2009**, *24*, 26−35.
(11) Motterlini, R.; Otterbein, L. E. *Nat. Rev. Drug. Discovery* **2010**, *9*, 728−743.
(12) Romao, C. C.; Blättler, W. A.; Seixas, J. D.; Bernardes, G. J. L. *Chem. Soc. Rev.* **2012**, *41*, 3571−3583.
(13) Mann, B. E. Carbon monoxide: An essential signalling molecule. In *Topics in Organometallic Chemistry*; Metzler-Nolte, N., Jaouen, G., Eds.; Springer: Berlin, 2010; Vol. *32*, pp 247−285.
(14) Johnson, T. R.; Mann, B. E.; Clark, J. E.; Foresti, R.; Green, C. J.; Motterlini, R. *Angew. Chem., Int. Ed.* **2003**, *42*, 3722−3729.
(15) Motterlini, R.; Mann, B. E.; Johnson, T. R.; Clark, J. E.; Foresti, R.; Green, C. J. *Curr. Pharm. Des.* **2003**, *9*, 2525−2539.
(16) Motterlini, R.; Mann, B. E.; Foresti, R. *Expert Opin. Invest. Drugs* **2005**, *14*, 1305−1318.
(17) Boczkowski, J.; Poderoso, J. J.; Motterlini, R. *Trends Biochem. Sci.* **2006**, *31*, 614−621.
(18) Mann, B. E.; Motterlini, R. *Chem. Commun.* **2007**, 4197−4208.
(19) Alberto, R.; Motterlini, R. *Dalton Trans.* **2007**, 1651−1660.
(20) Fairlamb, I. J. S.; Lynam, J. M.; Moulton, B. E.; Taylor, I. E.; Duhme-Klair, A.-K.; Sawle, P.; Motterlini, R. *Dalton Trans.* **2007**, 3603−3605.
(21) Atkin, A. J.; Williams, S.; Motterlini, R.; Lynam, J. M.; Fairlamb, I. J. S. *Dalton Trans.* **2009**, 3653−3656.
(22) Zhang, W. Q.; Atkin, A. J.; Thatcher, R. J.; Whitwood, A. C.; Fairlamb, I. J. S.; Lynam, J. M. *Dalton Trans.* **2009**, 4351−4358.
(23) Zhang, W.-Q.; Whitwood, A. C.; Fairlamb, I. J. S.; Lynam, J. M. *Inorg. Chem.* **2010**, *49*, 8941−8952.
(24) Marques, A. R.; Kromer, L.; Gallo, D. J.; Penacho, N.; Rodrigues, S. S.; Seixas, J. D.; Bernardes, G. J. L.; Reis, P. M.; Otterbein, S. L.; Ruggieri, R. A.; Goncalves, A. S. G.; Goncalves, A. M. L.; De Matos, M. N.; Bento, I.; Otterbein, L. E.; Blättler, W. A.; Romao, C. C. *Organometallics* **2012**, *31*, 5810−5822.
(25) Schatzschneider, U. *Eur. J. Inorg. Chem.* **2010**, 1451−1467.
(26) Schatzschneider, U. *Inorg. Chim. Acta* **2011**, *374*, 19−23.
(27) Rimmer, R. D.; Pierri, A. E.; Ford, P. C. *Coord. Chem. Rev.* **2012**, *256*, 1509−1519.
(28) Johnson, T. R.; Mann, B. E.; Teasdale, I. P.; Adams, H.; Foresti, R.; Green, C. J.; Motterlini, R. *Dalton Trans.* **2007**, 1500−1508.
(29) Hewison, L.; Crook, S. H.; Johnson, T. R.; Mann, B. E.; Adams, H.; Plant, S. E.; Sawle, P.; Motterlini, R. *Dalton Trans.* **2010**, *39*, 8967−8975.
(30) Gonzalez, M. A.; Fry, N. L.; Burt, R.; Davda, R.; Hobbs, A.; Mascharak, P. K. *Inorg. Chem.* **2011**, *50*, 3127−3134.
(31) Romanski, S.; Kraus, B.; Schatzschneider, U.; Neudörfl, J.; Amslinger, S.; Schmalz, H.-G. *Angew. Chem., Int. Ed.* **2011**, *50*, 2392−2396.
(32) Romanski, S.; Rücker, H.; Stamellou, E.; Guttentag, M.; Neudörfl, J.; Alberto, R.; Amslinger, S.; Yard, B.; Schmalz, H.-G. *Organometallics* **2012**, *31*, 5800−5809.
(33) Romanski, S.; Kraus, B.; Guttentag, M.; Schlundt, W.; Rücker, H.; Adler, A.; Neudörfl, J.-M.; Alberto, R.; Amslinger, S.; Schmalz, H.-G. *Dalton Trans.* **2012**, *41*, 13862−13875.
(34) Niesel, J.; Pinto, A.; Peindy N'Dongo, H. W.; Merz, K.; Ott, I.; Gust, R.; Schatzschneider, U. *Chem. Commun.* **2008**, 1798−1800.
(35) Pfeiffer, H.; Rojas, A.; Niesel, J.; Schatzschneider, U. *Dalton Trans.* **2009**, 4292−4298.
(36) Crook, S. H.; Mann, B. E.; Meijer, A. J. H. M.; Adams, H.; Sawle, P.; Scapens, D.; Motterlini, R. *Dalton Trans.* **2011**, *40*, 4230−4235.
(37) Kunz, P. C.; Huber, W.; Rojas, A.; Schatzschneider, U.; Spingler, B. *Eur. J. Inorg. Chem.* **2009**, 5358−5366.
(38) Brückmann, N. E.; Wahl, M.; Reiß, G. J.; Kohns, M.; Wätjen, W.; Kunz, P. C. *Eur. J. Inorg. Chem.* **2011**, 4571−4577.
(39) Huber, W.; Linder, R.; Niesel, J.; Schatzschneider, U.; Spingler, B.; Kunz, P. C. *Eur. J. Inorg. Chem.* **2012**, 3140−3146.
(40) Mohr, F.; Niesel, J.; Schatzschneider, U.; Lehmann, C. W. *Z. Anorg. Allg. Chem.* **2012**, *638*, 543−546.
(41) Pfeiffer, H.; Sowik, T.; Schatzschneider, U. *J. Organomet. Chem.* **2013**, *734*, 17−24.
(42) Zobi, F.; Degonda, A.; Schaub, M. C.; Bogdanova, A. Y. *Inorg. Chem.* **2010**, *49*, 7313−7322.
(43) Zobi, F.; Blacque, O. *Dalton Trans.* **2011**, *40*, 4994−5001.
(44) Bikiel, D. E.; Solveyra, E. G.; Di Salvo, F.; Milagre, H. M. S.; Eberlin, M. N.; Correa, R. S.; Ellena, J.; Estrin, D. A.; Doctorovich, F. *Inorg. Chem.* **2011**, *50*, 2334−2345.
(45) Alberto, R.; Ortner, K.; Wheatley, N.; Schibli, R.; Schubiger, A. P. *J. Am. Chem. Soc.* **2001**, *123*, 3135−3136.
(46) Motterlini, R.; Sawle, P.; Bains, S.; Hammad, J.; Alberto, R.; Foresti, R.; Green, C. J. *FASEB J.* **2004**, *18*, 284−286.

(47) Pitchumony, T. S.; Spingler, B.; Motterlini, R.; Alberto, R. *Chimia* **2008**, *62*, 277−279.
(48) Pitchumony, T. S.; Spingler, B.; Motterlini, R.; Alberto, R. *Org. Biomol. Chem.* **2010**, *8*, 4849−4954.
(49) Dördelmann, G.; Pfeiffer, H.; Birkner, A.; Schatzschneider, U. *Inorg. Chem.* **2011**, *50*, 4362−4367.
(50) Dördelmann, G.; Meinhardt, T.; Sowik, T.; Krüger, A.; Schatzschneider, U. *Chem. Commun.* **2012**, *48*, 11528−11530.
(51) Rimmer, R. D.; Richter, H.; Ford, P. C. *Inorg. Chem.* **2010**, *49*, 1180−1185.
(52) Kretschmer, R.; Gessner, G.; Görls, H.; Heinemann, S. H.; Westerhausen, M. *J. Inorg. Biochem.* **2011**, *105*, 6−9.
(53) Jackson, C. S.; Schmitt, S.; Dou, Q. P.; Kodanko, J. J. *Inorg. Chem.* **2011**, *50*, 5336−5338.
(54) Pierri, A. E.; Pallaoro, A.; Wu, G.; Ford, P. C. *J. Am. Chem. Soc.* **2012**, *134*, 18197−18200.
(55) Gonzalez, M. A.; Carrington, S. J.; Fry, N. L.; Martinez, J. L.; Mascharak, P. K. *Inorg. Chem.* **2012**, *51*, 11930−11940.
(56) Gonzalez, M. A.; Yim, M. A.; Cheng, S.; Moyes, A.; Hobbs, A. J.; Mascharak, P. K. *Inorg. Chem.* **2012**, *51*, 601−608.
(57) Szacilowski, K.; Macyk, W.; Drzewiecka-Matuszek, A.; Brindell, M.; Stochel, G. *Chem. Rev.* **2005**, *105*, 2647−2694.
(58) Agostinis, P.; Berg, K.; Cengel, K. A.; Foster, T. H.; Girotti, A. W.; Gollnick, S. O.; Hahn, S. M.; Hamblin, M. R.; Juzeniene, A.; Kessel, D.; Korbelik, M.; Moan, J.; Mroz, P.; Nowis, D.; Piette, J.; Wilson, B. C.; Golab, J. *Cancer J. Clin.* **2011**, *61*, 250−281.
(59) Juris, A.; Balzani, V.; Barigelletti, F.; Campagna, S.; Belser, P.; Von Zelewsky, A. *Coord. Chem. Rev.* **1988**, *84*, 85−277.
(60) Rutherford, T. J.; Reitsma, D. A.; Keene, F. R. *Dalton Trans.* **1994**, 3659−66.
(61) Spiccia, L.; Deacon, G. B.; Kepert, C. M. *Coord. Chem. Rev.* **2004**, *248*, 1329−1341.
(62) Eskelinen, E.; Haukka, M.; Venaelaeinen, T.; Pakkanen, T. A.; Wasberg, M.; Chardon-Noblat, S.; Deronzier, A. *Organometallics* **2000**, *19*, 163−169.
(63) Eskelinen, E.; Luukkanen, S.; Haukka, M.; Ahlgren, M.; Pakkanen, T. A. *Dalton Trans.* **2000**, 2745−2752.
(64) Eskelinen, E.; Kinnunen, T.-J. J.; Haukka, M.; Pakkanen, T. A. *Eur. J. Inorg. Chem.* **2002**, 1169−1173.
(65) Gabrielsson, A.; Zalis, S.; Matousek, P.; Towrie, M.; Vlcek, A. *Inorg. Chem.* **2004**, *43*, 7380−7388.
(66) Gabrielsson, A.; Towrie, M.; Zalis, S.; Vlcek, A. *Inorg. Chem.* **2008**, *47*, 4236−4242.
(67) Schubert, U. S.; Eschbaumer, C.; Hien, O.; Andres, P. R. *Tetrahedron Lett.* **2001**, *42*, 4705−4707.
(68) Badger, G. M.; Sasse, W. H. F. *J. Chem. Soc.* **1956**, 616−620.
(69) Peek, B. M.; Ross, G. T.; Edwards, S. W.; Meyer, G. J.; Meyer, T. J.; Erickson, B. W. *Int. J. Pept. Protein Res.* **1991**, *38*, 114−23.
(70) Nickita, N.; Gasser, G.; Pearson, P.; Belousoff, M. J.; Goh, L. Y.; Bond, A. M.; Deacon, G. B.; Spiccia, L. *Inorg. Chem.* **2008**, *48*, 68−81.
(71) Gholamkhass, B.; Koike, K.; Negishi, N.; Hori, H.; Takeuchi, K. *Inorg. Chem.* **2001**, *40*, 756−765.
(72) Thomson, S. A.; Josey, J. A.; Cadilla, R.; Gaul, M. D.; Fred Hassman, C.; Luzzio, M. J.; Pipe, A. J.; Reed, K. L.; Ricca, D. J.; Wiethe, R. W.; Noble, S. A. *Tetrahedron* **1995**, *51*, 6179−6194.
(73) Dutta, S.; Kim, S.-K.; Patel, D. B.; Kim, T.-J.; Chang, Y. *Polyhedron* **2007**, *26*, 3799−3809.
(74) Anderson, P. A.; Deacon, G. B.; Haarmann, K. H.; Keene, F. R.; Meyer, T. J.; Reitsma, D. A.; Skelton, B. W.; Strouse, G. F.; Thomas, N. C. *Inorg. Chem.* **1995**, *34*, 6145−6157.
(75) Nickita; Belousoff, M. J.; Bhatt, A. I.; Bond, A. M.; Deacon, G. B.; Gasser, G.; Spiccia, L. *Inorg. Chem.* **2007**, *46*, 8638−8651.
(76) Gottlieb, H. E.; Kotlyar, V.; Nudelman, A. *J. Org. Chem.* **1997**, *62*, 7512−7515.
(77) Fulmer, G. R.; Miller, A. J. M.; Sherden, N. H.; Gottlieb, H. E.; Nudelman, A.; Stoltz, B. M.; Bercaw, J. E.; Goldberg, K. I. *Organometallics* **2010**, *29*, 2176−2179.
(78) Strouse, G. F.; Anderson, P. A.; Schoonover, J. R.; Meyer, T. J.; Keene, F. R. *Inorg. Chem.* **1992**, *31*, 3004−6.
(79) Gibson, D. H.; Sleadd, B. A.; Mashuta, M. S.; Richardson, J. F. *Organometallics* **1997**, *16*, 4421−4427.
(80) Atkin, A. J.; Lynam, J. M.; Moulton, B. E.; Sawle, P.; Motterlini, R.; Boyle, N. M.; Pryce, M. T.; Fairlamb, I. J. S. *Dalton Trans.* **2011**, *40*, 5755−5761.
(81) McLean, S.; Mann, B. E.; Poole, R. K. *Anal. Biochem.* **2012**, *427*, 36−40.
(82) Antonini, E.; Brunori, M. Hemoglobin and myoglobin their reactions with ligands. In *Frontiers of Biology*; Neuberger, A., Tatum, E. L., Eds.; North-Holland: Amsterdam, 1971; Vol. *21*.
(83) Hatchard, C. G.; Parker, C. A. *Proc. R. Soc. London A* **1956**, *235*, 518−536.
(84) Parker, C. A. *Proc. R. Soc. London A* **1953**, *220*, 104−116.
(85) Kuhn, H. J.; Braslavsky, S. E.; Schmidt, R. *Pure Appl. Chem.* **2004**, *76*, 2105−2146.
(86) Sauers, R. R.; van Arnum, S. A.; Scimone, A. A. *Green Chem.* **2004**, *6*, 578−582.
(87) Deacon, G. B.; Patrick, J. M.; Skelton, B. W.; Thomas, N. C.; White, A. H. *Aust. J. Chem.* **1984**, *37*, 929−945.
(88) Collomb-Dunand-Sauthier, M.-N.; Deronzier, A.; Ziessel, R. *J. Organomet. Chem.* **1993**, *444*, 191−198.
(89) Gabrielsson, A.; Záliš, S.; Matousek, P.; Towrie, M.; Vlček, A. *Inorg. Chem.* **2004**, *43*, 7380−7388.
(90) Kelly, J. M.; O'Connell, C. M.; Vos, J. G. *Dalton Trans.* **1986**, 253−258.
(91) Basolo, F.; Gray, H. B.; Pearson, R. G. *J. Am. Chem. Soc.* **1960**, *82*, 4200−4203.
(92) Lindoy, L. F.; Livingstone, S. E. *Coord. Chem. Rev.* **1967**, *2*, 173−193.
(93) Hammarström, L.; Johansson, O. *Coord. Chem. Rev.* **2010**, *254*, 2546−2559.
(94) Gasser, G.; Sosniak, A. M.; Metzler-Nolte, N. *Dalton Trans.* **2011**, *40*, 7061−7076.